Science of the Total Environment 665 (2019) 125–132

Contents lists available at ScienceDirect

Science of the Total Environment

journal homepage: www.elsevier.com/locate/scitotenv

Quantification of particulate matter, tracking the origin and relationship between elements for the environmental monitoring of the Antarctic region

J.O. Cáceres [a,*], D. Sanz-Mangas [a], S. Manzoor [a], L.V. Pérez-Arribas [a], J. Anzano [b]

[a] Laser Chemistry Research Group, Department of Analytical Chemistry, Faculty of Chemistry, Complutense University of Madrid. Plaza de Ciencias 1, 28040 Madrid, Spain
[b] Laser Lab, Chemistry & Environment Group, Department of Analytical Chemistry, Faculty of Sciences, University of Zaragoza. Pedro Cerbuna 12, 50009 Zaragoza, Spain

HIGHLIGHTS

- Particulate matter PM_{10} in Antarctic region (Deception Island) was analyzed.
- Low volume sampler was used to capture the aerosol particles (PM_{10}).
- Enrichment factors of Pb, Cr, Cu and Zn were calculated.
- Statistical tools were used to establish the correlations between the elements.
- Polar Contour Maps were used to determine the origin of pollutants

GRAPHICAL ABSTRACT

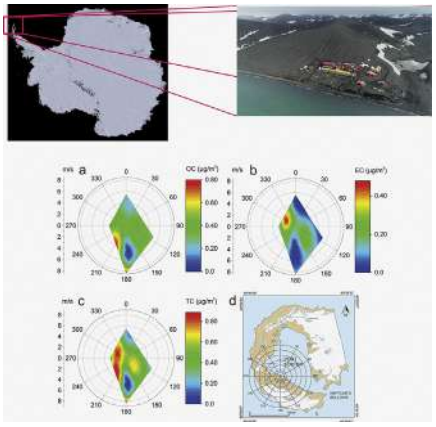

ARTICLE INFO

Article history:
Received 22 November 2018
Received in revised form 31 January 2019
Accepted 7 February 2019
Available online 08 February 2019

Editor: Jay Gan

Keywords:
Antarctic region
Deception Island
Atmospheric aerosols
Particulate matter
Enrichment factors
Polar contour maps

ABSTRACT

The present work reports on the analysis of atmospheric aerosols in the Antarctic region, Deception Island, collected during austral summer 2016–2017 by field measurements carried from Gabriel de Castilla Spanish Research Station. A low-volume sampler was used to capture the aerosols depositing them onto the air filters. A chemical analysis of the samples using Inductively Coupled Plasma-Mass Spectrometry (ICP-MS) and Inductively Coupled Plasma-Atomic Emission Spectroscopy (ICP-AES) provided the total carbon (TC), organic carbon (OC), elemental Carbon (EC) and elements such as Al, Ca, Fe, K, Mg, Na, P, S, Cu, Pb, Sr, Ti, Zn and Cr. The average mass concentration of particulate matter (PM_{10}) originated by natural and anthropogenic activities was calculated as $10 \pm 4\ \mu g/m^3$, although values such as $28.2\ \mu g/m^3$ were also obtained which is very high even when compared to other places in the coast of the Antarctic region. In addition, high enrichment factors have been found for elements such as Pb, Cr, Cu and Zn showing a remote anthropogenic contribution to particulate matter in this region. Correlations were found between Na, Mg, Ca, Al, Ti and S, where Na/Mg displayed the influence of marine environments, S correspond to volcanic activities, Ca to penguin colonies and influence of sea whereas Al/Ti indicated the crustal origin. Polar contour graphical maps were obtained from meteorological data using chemometrics methods, which allowed reproducing wind maps revealing the distribution of the aerosols and possible emission sources of different elements in the area. Given that this island has not been previously studied

* Corresponding author.
E-mail address: jcaceres@ucm.es (J.O. Cáceres).

https://doi.org/10.1016/j.scitotenv.2019.02.116
0048-9697/© 2019 Elsevier B.V. All rights reserved.

for atmospheric contamination, this work provides an interesting insight about the site-specific characteristics of particulate matter.

© 2019 Elsevier B.V. All rights reserved.

1. Introduction

The study of atmospheric aerosols plays a crucial role in understanding the impacts on the environment as a result of contamination (Bargagli, 2008). The scientific community has been studying the importance of these particles due to their effects on climate and health (Bellouin et al., 2005; Budhavant et al., 2017). The emission of contaminants into the troposphere directly affects remote places that are more vulnerable. Therefore, even protected places like Polar Regions face a progressive increase in the exposure to contaminants. The analytical studies of atmosphere provide information on aerosols affecting the environment and ecosystems. Atmospheric aerosols are liquid and/or solid particulate matter suspended in the atmosphere that enter there by natural or anthropogenic means (Budhavant et al., 2015; Huang et al., 2018; Putaud et al., 2010), including windborne crustal particles, sea salt oceanic spray, emissions from volcanoes and biomass burning (Brooks et al., 2008; Escudero et al., 2016; Nriagu, 1989; Shi et al., 2015; Xu et al., 2018). Aerosols have heterogeneous composition, variable size and can act as nuclei for the condensation of clouds (indirect effects), as well as disperse and absorb radiation (direct effects).

The latitude of Antarctic region and its surrounding ocean make it a trap for particulate matter imported from other latitudes (Bargagli, 2016; Eisele et al., 2008). Since the Antarctic region has unique conditions and is one of the unaltered and natural places, it offers valuable information about the circulation of atmospheric aerosols. The particulate matter is mostly composed by typically terrestrial crust and marine elements like Mn, Li, K, Al, Na, Fe and Mg and Rb in smaller proportions (Barbaro et al., 2016). Carbonaceous aerosols can be divided into different components like elemental carbon (EC) and organic carbon (OC). These carbonaceous particles absorb and scatter the radiation directly affecting the radioactive balance of the Earth (Bond and Bergstrom, 2006; Escudero et al., 2015). EC is basically graphite produced by combustion of fossil coal or gas (Fuzzi et al., 2006). On the other hand, OC can be emitted directly to the atmosphere or formed by photooxidative processes (Karanasiou et al., 2010).

Modelling relationships between different analytical data based on chemometrics allows simulating the temporal and spatial variations in complex terrains (Cristofanelli et al., 2018; Godfrey and Clarkson, 1998; Mihalikova and Kirkwood, 2013), performing an evaluation to detect groups of data and their relationships. Among the most common methods to analyze datasets, one of the most useful is the multivariate statistical technique, which allows to deal with massive amount of environmental data (Pérez-Arribas et al., 2017).

To the best of our knowledge, there are no studies on atmosphere composition and its origin in the Deception Island, despite the importance that aerosols play in air quality and climate. Furthermore, the studies on the Antarctic atmospheric aerosols have been carried out at locations far away from Deception Island, such as Terra Nova Bay (Annibaldi et al., 2007; Barbaro et al., 2016; Bazzano et al., 2015; Frydenvang et al., 2013), Dumont d'Urville Station, Petrel Island (Wolff et al., 1998). Due to this fact, there are no data available for aerosol composition and origin in this region. Hence, the aim of this work was to analyze the particulate matter of Deception Island in order to study its elemental composition for the characterization of the aerosols, looking for anthropogenic and natural sources of such elements on the Antarctic coastal environment. Natural or anthropogenic sources of on the measured elemental concentration were evaluated through the enrichment factors (EF). Furthermore, combination of statistical and graphical approaches is proposed to establish the relationship between the constituent elements and their concentration in order to reveal the influence of sea interaction, anthropogenic activities, penguin colonies and volcanic activity in this Antarctic region.

2. Material and methods

2.1. Geographical setting

Deception Island (Fig. 1), located at 62°58′09″S 60°42′33″W, is one of the three emerged volcanoes located in the Bransfield Strait, Antarctic zone. The island is a stratovolcano of approximately 15 km in diameter and is part of a volcanic complex situated at South-West in the archipelago of the Shetlands on South.

Meteorological data obtained during austral summer 2016–2017 on Deception Island by Gabriel de Castilla Spanish Research station reported a relative humidity of 64–97% and a temperature of −1 to 8 °C, respectively. The average wind speed was 3.59 m/s and the direction was from the south through the entrance of the bay called Neptune's Bellows situated about 5 km from sampling point. Approximately 60% of the surface of the island is permanently covered by snow.

2.2. Sampling and processing

The PM_{10} samples were collected daily in the summer of 2016–2017 (from Dec. to Feb.) using a low-volume sampler (2.3 m^3/h) model Derenda LVS 3.1, equipped with a European Union reference PM_{10} inlet. Circular quartz microfiber filter of 47 mm diameter (Munktell) was used. Each sample was collected during 24 h during the days when the atmospheric conditions were suitable. A total of 37 samples was collected, where 15 of them were suitable for the analysis. The remaining samples were discarded as no difference in mass was observed in gravimetric analysis. Alternatively, random top soil samples were recollected near the sampling point. After the determination of PM_{10}, mass concentrations were obtained by gravimetry according to European Norm (DIN-EN-12341, 2014) and a chemical characterization of the samples was carried out following the analytical procedure published by Querol et al. (1996)). Al, Ca, Fe, K, Mg, Na, P, S, Cu, Pb, Sr, Ti, Zn and Cr were investigated. A half of the filter papers were cut and digested with 2.5 mL of HNO_3 at 65%, 5 mL of HF at 40% to dissolve aluminosilicates, carbonates, sulfur, etc., And finally 2.5 mL of 60% $HClO_4$ to dissolve organic matter. A circular punch of 1 in. in diameter was analyzed for total carbon (TC) with an elemental LECO analyzer, and a 1.5 cm^2 rectangular punch was analyzed by a thermal-optical method (Sunset OCEC Analyzer) to obtain the organic carbon (OC) and elemental carbon (EC) in the particulate matter, following a modified temperature protocol (NIOSH, 2003) and EUSAAR2 software (Bautista et al., 2015). The OC + EC analysis was made under a quality system based on European Standards and International Organization for Standardization and by the International Electro-technical Commission (ISO/IEC-17025, 2005) standard. After the total carbon analysis, the concentrations of CO_3^{2-} and SiO_2 were calculated indirectly from the concentrations of Ca, Mg and Al. The non-mineral carbon (C_{nm}) was obtained from the difference between TC and carbon in CO_3^{2-}. OM (organic matter) was calculated from OC by applying a factor of 1.8 (Turpin et al., 2000).

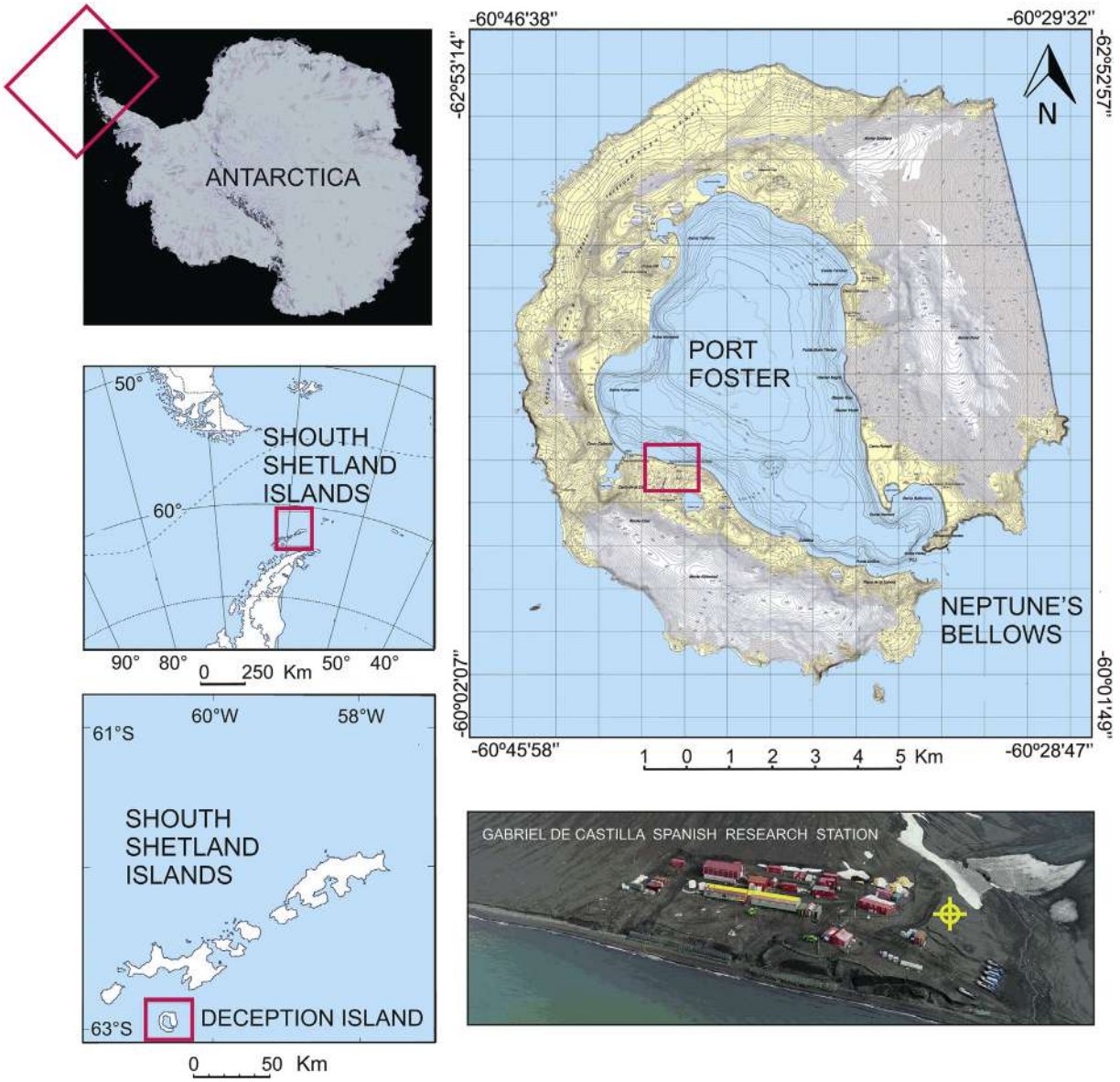

Fig. 1. Map of Deception Island with the location of Gabriel de Castilla Spanish Research Station. The yellow marker shows the position of the low volume sampler. Images taken from LANDSAT, Geographical maps by the Ministry of Defense of Spain. (For interpretation of the references to colour in this figure legend, the reader is referred to the web version of this article.)

2.3. ICP-MS and ICP-AES set-up

ICP-MS model X-Series II (Brand: Thermo Fisher scientific) with a quadruple analyzer was used for the quantitative elemental analysis of Cu, Pb, Sr, Ti, Zn and Cr. An external calibration was done using blank filters and certified standards of fly ash International Reference Material NBS1633b from National Institute of Standards and Technology (NIST) similar in composition to the particulate materials were analyzed following the same procedure for quality assurance and control. These standards cover the entire range of expected concentrations forming the calibration lines (0.5–100 ng/mL). Internal correction was made by using 10 ng/mL of In as an internal standard. The quantification limit (LOQ) of ICP-MS was determined as 0.2 ng/mL.

The ICP-AES (Brand: Thermo Fisher Scientific) was a cap 6500 Radial Model, used for simultaneous analysis of major and trace elements in the same samples, concretely Al, Ca, Fe, K, Mg, Na, P and S. Through an optical system composed of an Echelle network, the emitted radiation is resolved, and this is detected by Charge Injection Device (CID). The configuration of this equipment works with micro flow nebulizer mounted in a cyclonic nebulization chamber and CID detector composed of 540 × 540 pixels with a previous prism of 21°, measuring wavelengths from 166 to 847 nm. The same procedure and standard reference material were used to ICP-AES measurements for quality assurance and control. The LOQ calculated was better than 0.05 μg/m^3 for all elements, reaching to 0.001 μg/m^3 for the most sensitive elements (cases of Mn, Sr and Ba).

2.4. Data processing

The study of the relationship between different elements was carried out through the statistical methods of multivariate analysis of correlation coefficients. Correlation Analysis provides information about the association and modelling of the variations of elements present in the air particulate matter. Multidimensional analysis allows establishing correlations between the elements in the aerosols and has been applied in several studies to identify sources of chemical components (Zhu et al., 2017). Principal component analysis (PCA) uses the correlation

between the data and is based on the reduction of big dataset down to the smaller parts. This method represents a simplification of the position of the elements in a reduced coordinate system (Pérez-Arribas et al., 2017) and has been proven to be a very useful tool for large datasets interpretation in other fields (Mostert et al., 2010; Reinholds et al., 2015). Factor analysis has also been used in order to express data as functions to describe the variability among the correlated variables. In this work, Statgraphics Centurion 18, version 18.1.06 of 64-bits (Statpoint Technologies, Warrenton, Virginia) was used for performing Correlation Analysis, PCA and Factor Analysis.

Polar contour maps represent a useful procedure for data visualization. The use of wind direction and speed offer a simple and useful plot of air-pollutants sources. The wind speed is in the x-axis (The radius in degrees), wind direction in the y-axis of the angle and concentration in z-axis, that control the contour of data and their relationships were found using OriginPro 2017, 64-bit (OriginLab Corporation, Northampton, Massachusetts, EEUU).

3. Results and discussion

The values of the particulate matter show an average result of 10 ± 4 μg/m^3, which is a value similar to that obtained for PM_{10} in rural areas and of low population density (Escudero et al., 2016). In addition, this value is comparable to mass average in places such as the Southern Ocean with an average value of 13.4 μg/m^3 (Budhavant et al., 2015), in contrast to other places on the Antarctic coast, where the average was 1.5 μg/m^3 or 3.4 μg/m^3 (Budhavant et al., 2017; Mazzera et al., 2001). However, during some days the measured concentrations in the filters were surprisingly high such as 28.20, 21.70 and 19.52 μg/m^3. Table 1 shows the concentrations obtained per day by the low volume sampler.

3.1. Enrichment factor

In order to investigate the influence of natural or anthropogenic sources on the measured elemental concentration, enrichment factors (EF) were calculated according to the equation:

$$EF = \left(\frac{X}{Ref}\right) aerosol / \left(\frac{X}{Ref}\right) soil$$

where X is the concentration of evaluating element and *Ref* is the corresponding concentration of the element used as a reference (Winchester et al., 1981). Since Al and Ti are common constituents of the Earth's crust they have been used as tracers for crustal aerosols. Crustal composition of the soils shows concentration of 88.75, 65.55, 10.13, 0.442, 0.487, 0.145 and 0.0029 mg/kg for Al, Ti, Cr, Cu, Zn, and Pb, respectively. Also the PM10 composition was 0.025, 0.0055, 0.0046 and 0.0019 mg/m^3 for Cr, Cu, Zn and Pb, respectively, showing very high EF values (Table 2), indicating anthropogenic pollution. These high values of EF and pollutants have been attributed to remote anthropogenic sources from the upper atmosphere (Annibaldi et al., 2007). Furthermore, the diesel generator installed at the research base can be responsible for part of the presence of these elements.

These results are in good agreement with previous investigations of trace metals in Antarctic aerosols referred to anthropogenic activities, however the values of Cr are higher while Pb is lower compared with other places like Terra Nova Bay (Bazzano et al., 2015).

Table 1
PM_{10}, humidity, wind direction, speed and average daily temperature during the collection period.

Date	PM_{10} (μg/m^3)	Humidity (%)	Wind direction	Wind speed (m/s)	Average daily temperature (°C)
28/12/16	6.2	64.0	E-SE	2.4	1.2
30/12/16	28.2	65.5	S-SE	5.2	−0.4
01/01/17	21.7	67.0	W-NW	2.8	1.7
07/01/17	8.1	80.0	E	5.8	2.1
21/01/17	12.2	90.5	E-NE	3.4	1.6
22/01/17	2.9	86.0	N-E	1.1	5.1
23/01/17	9.4	72.5	E	2.9	2.8
01/02/17	4.3	82.5	N	3.0	3.3
08/02/17	3.8	91.0	NW-N	1.9	3.6
14/02/17	2.9	92.5	–	2.3	2.3
17/02/17	4.7	88.0	–	1.9	3.3
23/02/17	12.1	87.5	W	3.8	2.3
24/02/17	19.5	86.0	W	5.5	3.8
25/02/17	7.4	77.0	–	3.0	3.9
26/02/17	6.0	96.5	E	8.4	−0.5

3.2. Multivariate analysis

Statistical analysis was performed on the data consisting of the major components of the aerosols. Meteorological variables like rain immediately before taking the sample, snowfall, wind, wind force or direction of the wind cannot explain the variability of the results between different days, ranging from 2.89 to 28.2 μg/m^3. In case of scarce rainfall, the erosion contributes to an increment of the particulate matter in the atmosphere, however, only this factor does not explain high values of PM_{10}. This variability was studied by performing a correlation analysis between the elements and by means of polar contour maps relating the windborne particles to the speed and direction of wind. Table 3 gives the correlation values between most representative elements, where the first row provides the Pearson coefficient (R); second row the number of samples and the third row gives the *P*-values. In addition, the more significant cases are highlighted.

Given that the main source of sodium is marine aerosols, and a high correlation ($R = 0.9978$) was found between Na and Mg, shows that Mg also has the same origin. This can be supported by the ratio of Na/Mg in seawater which is around 8.3, close to the value found in the particulate matter as 7.8 (mean values: 1.768 μg/m^3 for Na and 0.226 μg/m^3 for Mg).

The correlation between Ca (mean value 0.114 μg/m^3) and Na ($R = 0.8867$) and between Ca and Mg ($R = 0.8989$), were higher than the correlations of these elements with Al (mean value 0.059 μg/m^3), (Al/Ca = 0.7875, R for Al/Mg = 0.5290) which is a typical terrestrial element present in silicates. This implies that an important part of the Ca in the aerosols comes from the marine environment, as well as other biological sources such as shells, eggshell remains of the penguins and other nesting birds.

On the other hand, the high correlation between Al and Ti (mean values of Ti 0.114 μg/m^3 $R = 0.9369$) indicates a terrestrial origin, especially originating from volcanic soils and due to an erosive effect of wind. Another significant correlation was found among S (mean value 0.283 μg/m^3) and Ca ($R = 0.8814$), S with Mg ($R = 0.8582$) and S with Na ($R = 0.8426$). It is obvious that these relationships with S arise from the combination of marine and volcanic activity due to hydrothermal processes. This is produced by the fumarolic activity in inundated zones of the coast due to steam distilling phenomena. A significant correlation was found between K and P ($R = 0.9817$), which is separated from other elements, suggest a completely different source, indicating that they come from sources other than marine aerosols, soil erosion and biological matter essentially. The values of the Na/Mg ratio ranging from 6.42 to 8.38, shows an approximately constant behavior during the sampling period which is similar to the other element ratio.

Table 2
Enrichment factor in Gabriel de Castilla Spanish research base.

EF	Cr	Cu	Zn	Pb
Ti	690.2	12.5	38.0	79.8
Al	866.3	15.7	47.7	100.2

Table 3
Correlation values of representative elements indicating Pearson coefficient (italic), sample size (parenthesis) and *P*-value (bold).

	T. carb.	*Al*	*Ca*	*Fe*	*K*	*Mg*	*Na*	*P*	*S*	*Ti*
T. carb.		*0.4486* (14) **0.108**	*0.3047* (15) **0.270**	*0.1494* (12) **0.643**	*0.1292* (15) **0.646**	*0.0405* (15) **0.886**	*0.0017* (15) **0.995**	*0.0235* (13) **0.939**	*0.1352* (15) **0.631**	*0.5508* (15) **0.033**
Al			*0.7875* (14) **≤0.001**	*0.4708* (11) **0.144**	*0.1007* (14) **0.732**	*0.5290* (14) **0.052**	*0.4893* (14) **0.076**	*0.1943* (12) **0.545**	*0.7370* (14) **0.003**	*0.9369* (14) **≤0.001**
Ca				*0.5102* (12) **0.090**	*0.1411* (15) **0.616**	*0.8989* (15) **≤0.001**	*0.8867* (15) **≤0.001**	*0.0553* (13) **0.858**	*0.8814* (15) **≤0.001**	*0.7094* (15) **0.003**
Fe					*-0.2482* (12) **0.437**	*0.2910* (12) **0.359**	*0.2862* (12) **0.367**	*-0.2843* (11) **0.397**	*0.2375* (12) **0.457**	*0.3893* (12) **0.211**
K						*0.1427* (15) **0.612**	*0.1392* (15) **0.621**	*0.9817* (13) **≤0.001**	*0.0367* (15) **0.897**	*0.2082* (15) **0.457**
Mg							*0.9978* (15) **≤0.001**	*0.0298* (13) **0.923**	*0.8582* (15) **≤0.001**	*0.4257* (15) **0.114**
Na								*0.0286* (13) **0.926**	*0.8426* (15) **≤0.001**	*0.3816* (15) **0.161**
P									*0.0039* (13) **0.990**	*0.2618* (13) **0.388**
S										*0.6764* (15) **0.006**

The loading analysis from PCA (Fig.2) supports the correlation analysis, as commented previously. It can be seen that the weight vectors corresponding to Na and Mg are almost the same and are practically superimposed, which indicate the same origin of those elements. The presence of Ca, which appears between the Na and Al, indicate influence of both the marine aerosols and terrestrial erosion. A strong relationship between P and K was observed which can be seen from the loadings corresponding to these elements. However, at the same time they are present in an orthogonal position (an angle of 90°) with respect to Na, Mg, Fe, S and Ca, indicating that these elements are totally independent regarding their origin.

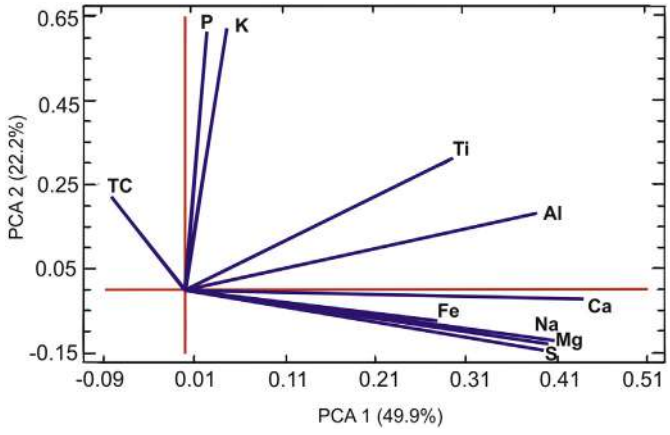

Fig. 2. Loading from statistical analysis of the samples by PCA of TC, Al, Ca, Fe, K, Mg, Na, P, S, Ti.

3.3. Polar contour maps

To study the influence of the meteorological parameters on the variability of the amount of the particulate matter, polar contour maps have been obtained in order to relate the windborne particles to the speed and direction of wind. The particulate matter of the aerosols combined with the direction of the wind is represented in Figs. 3 and 5.

Polar contour maps corresponding to total carbon (Fig. 3a) show two principal emission sources located approximately at the northwest and southwest of the sampling point. With the aim of a better visualization and verification, two additional contour maps were made for OC and EC separately (Fig. 3b, and c), that revealed the existence of two different origins for carbon. One corresponding to OC was located in the southwest, which showed that it originated from penguin colonies. The second source of carbon was EC, produced due to the combustion of fuels and it comes mainly from the research base located in the northwest of the sampling point. These different origins of OC and EC in particulate matter can be confirmed by a Factor Analysis (Fig. 4), where loading EC and OC are nearly in orthogonal directions, which indicates that they are independent sources of carbon production.

In the case of the other elements, the polar contour maps show that Mg and Na (Fig. 5a, & b) have the same source in the north, coming from the Foster bay as marine aerosols. The high concentrations from

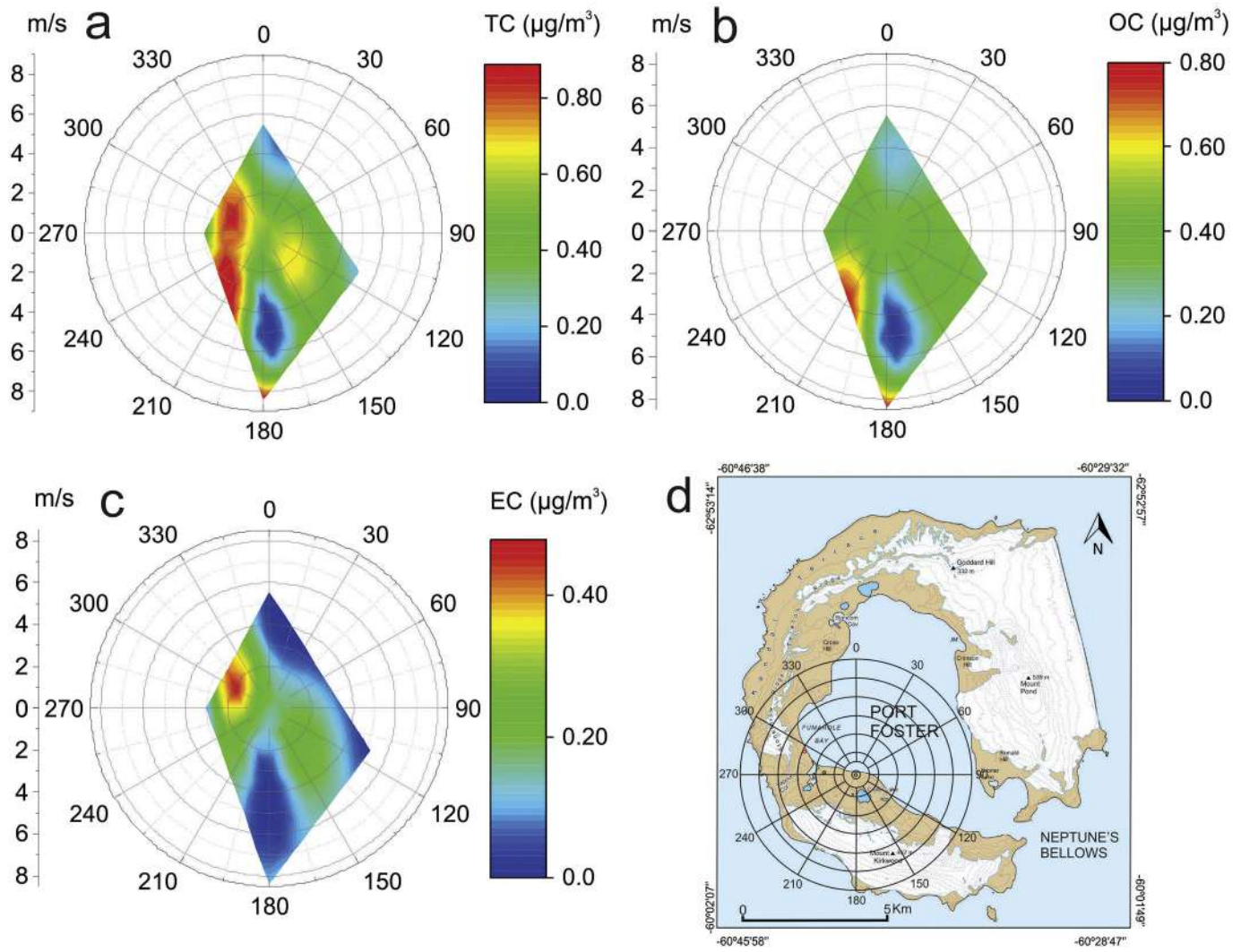

Fig. 3. Polar contour maps in relation to wind direction and speed for a) total carbon (TC), b) organic carbon (OC) and c) elemental carbon (EC) d) Geographical map with a compass rose showing the sampling point at Gabriel de Castilla Spanish Research base. (For interpretation of the references to colour in this figure legend, the reader is referred to the web version of this article.)

seawater sources demonstrate the importance of the influence of scavenging processes in coastal regions. The principal source of phosphorus (Fig. 5c) was guano-derived compound coming from the penguin colonies, located at the southwest of sampling point. Fig. 5d & 5e show that Ti and Al have the same source in the northwest, which is essentially caused by the erosion of the volcanic soil (Budhavant et al., 2015). In addition, Fig. 5f shows the source of sulfur in the north–northwest, where it is unexpectedly high. This fact can be attributed to the intense volcanic activity of Fumarole Bay that emits sulfur derivatives. The source and origin of Ca (Fig. 5g) lie in the same direction as that of Sulfur, which was also demonstrated by the correlation and PCA analysis, but also of Mg and Na. Thus, it is clear that its origin was fumarolic and marine, arising from the evaporation of sea water. Fe (Fig. 5h) presents a similar profile as that of Al and Ti but in lower concentration, with principal origin as crustal. Due to diverse composition and multiple sources of particulate matter, it is difficult to describe concretely its global origin, which can be seen from Fig. 5i, where the total particulate matter is scattered.

Fig. 5i shows the total PM_{10} (TPM_{10}) at a scale of 30 μg/m³. As can be seen, the highest levels come from the southeast and northwest essentially from sea (Foster bay). This increment of particulate matter can be explained because of the horseshoe shape of Deception Island. The seawater vapor increases the concentration of aerosols in the air due to the special orography surrounded by volcanic ridges around 500 m of altitude and not be scattered by the winds as it happens in open areas or near to other coastal places.

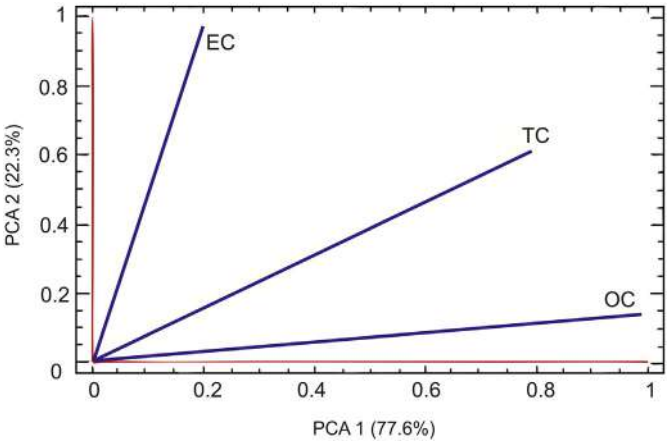

Fig. 4. Factor Analysis after varimax rotation for standardized TC, OC and EC variables.

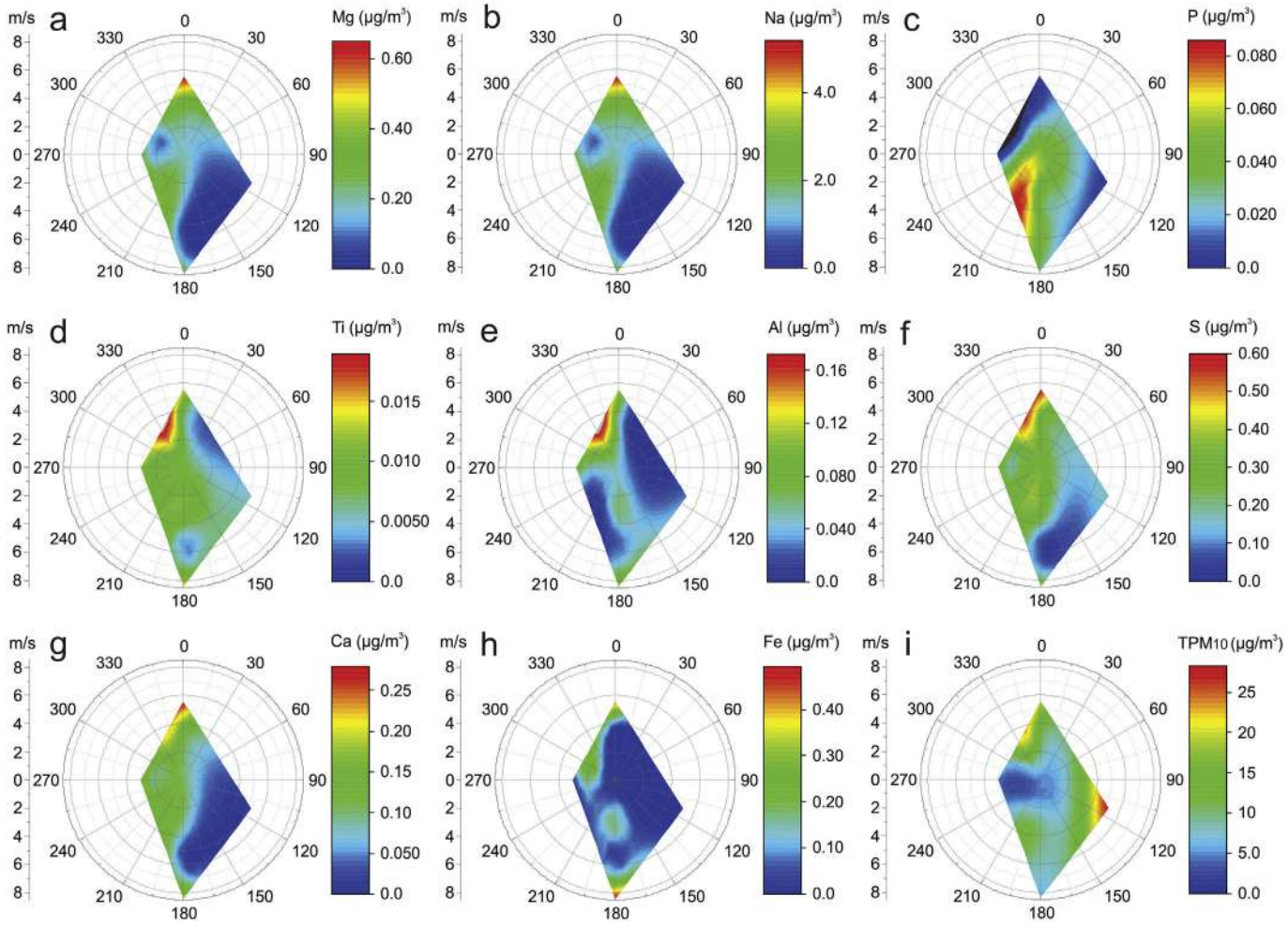

Fig. 5. Polar contour maps in relation to wind direction and speed for a) Mg; b) Na; c) P; d) Ti; e) Al; f) S; g) Ca; h) Fe; i) Total PM_{10} (TPM_{10}).

4. Conclusions

Field measurements were conducted during austral summer 2016–2017 on Deception Island carried out from the Gabriel de Castilla Spanish Research Station. The concentrations provided in this work reflect site-specific characteristics, which are shown during a short-time period in the austral summer. To our knowledge, these are the first aerosol measurements made at Deception Island at Gabriel de Castilla station and also the first application of polar contour maps for the evaluation of parameters of atmospheric particulate matter.

Polar contour maps showed the two principal emission sources of the TC, as located in the northwest and southwest of the sampling point. The OC was situated in the southwest and EC in the northwest of the sampling point. Thus, OC had its origin from penguin colonies, while EC was produced by the combustion of fuels, originated mainly from the research base located in the northwest of the sampling point. This has been confirmed by analysis of factors that showed a quasi-orthogonality between OC and EC. This polar contour map is also useful to find sources of particulate matter such as phosphorus coming from penguin colonies or sulfur from fumarolic activity.

The correlations between elements also confirmed the origin of the contaminants. The correlation between Na/Mg demonstrated the influence of sea since these elements originate from marine environments and have a strong presence in the seawater aerosols at coastal places. Ca/Na and Ca/Mg correlations indicate the aerosols from the marine environment, whereas Al/Ca and Al/Mg showed volcanic soil as their origin. On the other hand, the correlation S/Ca, S/Mg and S/Na result through the combination of hydrothermal activity in the sea, dragging the marine and Sulfur aerosols as a consequence of steam distillation, reflecting the intense volcanic activity in this region. K/P shows a completely different origin due to biological sources (organic matter and guano-derived elements). Finally, total PM_{10} windburn aerosols from the bay sustained the special conditions of Deception Island due to its extremely abrupt relief that blocks the dispersion of the wind. The given maps demonstrate their significance to assess possible emission sources of different elements.

The particulate matter measured during the campaign has a PM_{10} mass average (10 μg/m^3), which is higher as compared to other places on the coast of the Antarctic region. The highest value of PM_{10} found was 28.2 μg/m^3. This high value was attributed to the special horseshoe shape of the Deception Island, which maintains aerosols in the air for a longer time. Furthermore, the enrichment factors for the elements in the particulate matter such as Cr, Cu, Zn, and Pb, show the remote anthropogenic source of air pollution coming from the upper atmosphere into this Antarctic region.

The results give a clear view of particulate matter pollutants present in the air and show the importance of continuous monitoring of this region in future campaigns in order to expand this study. This effect marks the importance of a more comprehensive study of the atmospheric particulate matter in this Antarctic region. Further campaigns and analysis will be performed to get a deep understanding of the mechanisms and the results obtained.

Acknowledgements

The authors gratefully acknowledge the Complutense University of Madrid for facilities and material resources. This project forms part of the Ministry of Science, Innovation and Universities. Proposal # CTM2017-82929R in collaboration with the Government of Aragon. Proposal E23_17D. and financial support from European Social Found & University of Zaragoza. The geographic maps are provided with the consent of the Army Geographic Centre of the Ministry of Defense of Spain. Acknowledgement to the military members at the Gabriel de Castilla Spanish research base for help with the installation of equipment and sample collection. The data of ICP-MS and ICP-AES have been obtained in the Institute Environmental Assessment and Water Research, IDÆA.

Conflict of interest

The authors declare no conflict of interest.

References

Annibaldi, A., Truzzi, C., Illuminati, S., Bassotti, E., Scarponi, G., 2007. Determination of water-soluble and insoluble (dilute-HCl-extractable) fractions of Cd, Pb and Cu in Antarctic aerosol by square wave anodic stripping voltammetry: distribution and summer seasonal evolution at Terra Nova Bay (Victoria Land). Anal. Bioanal. Chem. 387, 977–998.

Barbaro, E., Zangrando, R., Kirchgeorg, T., Bazzano, A., Illuminati, S., Annibaldi, A., et al., 2016. An integrated study of the chemical composition of Antarctic aerosol to investigate natural and anthropogenic sources. Environ. Chem. 13, 867–876.

Bargagli, R., 2008. Environmental contamination in Antarctic ecosystems. Sci. Total Environ. 400, 212–226.

Bargagli, R., 2016. Atmospheric chemistry of mercury in Antarctica and the role of cryptogams to assess deposition patterns in coastal ice-free areas. Chemosphere 163, 202–208.

Bautista, A.T., Pabroa, P.C.B., Santos, F.L., Quirit, L.L., Asis, J.L.B., Dy, M.A.K., et al., 2015. Intercomparison between NIOSH, IMPROVE_A, and EUSAAR_2 protocols: finding an optimal thermal–optical protocol for Philippines OC/EC samples. Atmos. Pollut. Res. 6, 334–342.

Bazzano, A., Soggia, F., Grotti, M., 2015. Source Identification of Atmospheric Particle-bound Metals at Terra Nova Bay, Antarctica. vol. 12.

Bellouin, N., Boucher, O., Haywood, J., Reddy, M.S., 2005. Global estimate of aerosol direct radiative forcing from satellite measurements. Nature 438, 1138–1141.

Bond, T.C., Bergstrom, R.W., 2006. Light absorption by carbonaceous particles: an investigative review. Aerosol Sci. Technol. 40, 27–67.

Brooks, S., Lindberg, S., Southworth, G., Arimoto, R., 2008. Springtime atmospheric mercury speciation in the McMurdo, Antarctica coastal region. Atmos. Environ. 42, 2885–2893.

Budhavant, K., Safai, P.D., Rao, P.S.P., 2015. Sources and elemental composition of summer aerosols in the Larsemann Hills (Antarctica). Environ. Sci. Pollut. Res. 22, 2041–2050.

Budhavant, K.B., Rao, P.S.P., Safai, P.D., 2017. Size distribution and chemical composition of summer aerosols over Southern Ocean and the Antarctic region. J. Atmos. Chem. 74, 491–503.

Cristofanelli, P., Putero, D., Bonasoni, P., Busetto, M., Calzolari, F., Camporeale, G., et al., 2018. Analysis of multi-year near-surface ozone observations at the WMO/GAW "Concordia" station (75°06′S, 123°20′E, 3280 m a.S.L. – Antarctica). Atmos. Environ. 177, 54–63.

DIN-EN-12341, 2014. Ambient air - Standard gravimetric measurement method for the determination of the PM<(Index)10> or PM<(Index)2,5> mass concentration of suspended particulate matter. In: Standard, E. (Ed.), DIN EN 12341, p. 57.

Eisele, F., Davis, D.D., Helmig, D., Oltmans, S.J., Neff, W., Huey, G., et al., 2008. Antarctic Tropospheric Chemistry Investigation (ANTCI) 2003 overview. Atmos. Environ. 42, 2749–2761.

Escudero, M., Viana, M., Querol, X., Alastuey, A., Díez Hernández, P., García Dos Santos, S., et al., 2015. Industrial sources of primary and secondary organic aerosols in two urban environments in Spain. Environ. Sci. Pollut. Res. 22, 10413–10424.

Escudero, M., Lozano, A., Hierro, J., Tapia, O., del Valle, J., Alastuey, A., et al., 2016. Assessment of the variability of atmospheric pollution in National Parks of mainland Spain. Atmos. Environ. 132, 332–344.

Frydenvang, J., Kinch, K.M., Husted, S., Madsen, M.B., 2013. An optimized calibration procedure for determining elemental ratios using laser-induced breakdown spectroscopy. Anal. Chem. 85, 1492–1500.

Fuzzi, S., Andreae, M.O., Huebert, B.J., Kulmala, M., Bond, T.C., Boy, M., et al., 2006. Critical assessment of the current state of scientific knowledge, terminology, and research needs concerning the role of organic aerosols in the atmosphere, climate, and global change. Atmos. Chem. Phys. 6, 2017–2038.

Godfrey, J.J., Clarkson, T.S., 1998. Air quality modelling in a stable polar environment—Ross Island, Antarctica. Atmos. Environ. 32, 2899–2911.

Huang, J., Jaegle, L., Shah, V., 2018. Using CALIOP to constrain blowing snow emissions of sea salt aerosols over Arctic and Antarctic sea ice. Atmos. Chem. Phys. 18, 16253–16269.

ISO/IEC-17025, 2005. General requirements for the competence of testing and calibration laboratories. International Organization for Standardization.

Karanasiou, A., Diapouli, E., Viana, M., Alastuey, A., Querol, X., R., C., et al., 2010. On the Quantification of Atmospheric Carbonate Carbon by Thermal/Optical Analysis Protocol. vol. 4.

Mazzera, D.M., Lowenthal, D.H., Chow, J.C., Watson, J.G., Grubǐsíc, V., 2001. PM10 measurements at McMurdo Station, Antarctica. Atmos. Environ. 35, 1891–1902.

Mihalikova, M., Kirkwood, S., 2013. Tropopause Fold Occurrence Rates Over the Antarctic Station Troll (72° S, 2.5° E). vol. 31.

Mostert, M.M.R., Ayoko, G.A., Kokot, S., 2010. Application of chemometrics to analysis of soil pollutants. TrAC Trends Anal. Chem. 29, 430–445.

NIOSH, 2003. National Institute for Occupational Safety and Health 5040 method. Manual of Analytical Methods.

Nriagu, J.O., 1989. A global assessment of natural sources of atmospheric trace metals. Nature 338, 47.

Pérez-Arribas, L.V., León-González, M.E., Rosales-Conrado, N., 2017. Learning principal component analysis by using data from air quality networks. J. Chem. Educ. 94, 458–464.

Putaud, J.P., Van Dingenen, R., Alastuey, A., Bauer, H., Birmili, W., Cyrys, J., et al., 2010. A European aerosol phenomenology – 3: physical and chemical characteristics of particulate matter from 60 rural, urban, and kerbside sites across Europe. Atmos. Environ. 44, 1308–1320.

Querol, X., Alastuey, A., Lopez-Soler, A., Mantilla, E., Plana, F., 1996. Mineral composition of atmospheric particulates around a large coal-fired power station. Atmos. Environ. 30, 3557–3572.

Reinholds, I., Bartkevics, V., Silvis, I.C.J., van Ruth, S.M., Esslinger, S., 2015. Analytical techniques combined with chemometrics for authentication and determination of contaminants in condiments: a review. J. Food Compos. Anal. 44, 56–72.

Shi, G., Teng, J., Ma, H., Li, Y., Sun, B., 2015. Metals and Metalloids in Precipitation Collected During CHINARE Campaign From Shanghai, China to Zhongshan Station, Antarctica: Spatial Variability and Source Identification. vol. 29.

Turpin, B.J., Saxena, P., Andrews, E., 2000. Measuring and simulating particulate organics in the atmosphere: problems and prospects. Atmos. Environ. 34, 2983–3013.

Winchester, J.W., Weixiu, L., Lixin, R., Mingxing, W., Maenhaut, W., 1981. Fine and coarse aerosol composition from a rural area in north China. Atmos. Environ. 1967 (15), 933–937.

Wolff, E.W., Hall, J.S., Mulvaney, R., Pasteur, E.C., Wagenbach, D., Legrand, M., 1998. Relationship between chemistry of air, fresh snow and firn cores for aerosol species in coastal Antarctica. J. Geophys. Res.-Atmos. 103, 11057–11070.

Xu, G., Chen, L., Zhang, M., Zhang, Y., Wang, J., Lin, Q., 2018. Year-round records of bulk aerosol composition over the Zhongshan Station, Coastal East Antarctica. Air Qual. Atmos. Health, 1–18. https://doi.org/10.1007/s11869-018-0642-9.

Zhu, G., Guo, Q., Xiao, H., Chen, T., Yang, J., 2017. Multivariate statistical and lead isotopic analyses approach to identify heavy metal sources in topsoil from the industrial zone of Beijing Capital Iron and Steel Factory. Environ. Sci. Pollut. Res. 24, 14877–14888.